Available online at www.sciencedirect.com

SciVerse ScienceDirect

Procedia Engineering 34 (2012) 218 – 223

Procedia Engineering

www.elsevier.com/locate/procedia

9th Conference of the International Sports Engineering Association (ISEA)

# Multi-body power analysis of kicking motion based on a double pendulum

Hiroki Ozaki[a], Ken Ohta[b], Tsutomu Jinji[a]

[a]*Japan Institute of Sports Sciences, 3-15-1 Nishigaoka, Kita, Tokyo, 115-0056 Japan*
[b]*Keio Univercity, 5322 Endo, Fujisawa, Kanagawa, 252-0882 Japan*

Accepted 05 March 2012

**Abstract**

To kick a ball with the maximum velocity, the linear velocity of the kicking foot upon impact must be at the maximum. The dynamical mechanism of the kicking motion must be clarified to better understand the mechanism to produce the maximum velocity of the kicking foot. Therefore, the aim of this study was to clarify the mechanism that produces the maximum foot velocity using mathematical analysis based on a three-dimensional double pendulum model with a moving pivot. We investigated how the non-muscular forces of three components (i.e. centrifugal, Coriolis and gravity) generate, absorb, and transfer energy in order to produce the maximum swing velocity of the leg.



*Keywords:* Football; multi-body power analysis; double pendulum; energy flow

## 1. Introduction

The ball velocity of an instep kick depends on various factors including the foot mass of the kicking leg, the rigidity of the kicking foot, the impact point, and the linear velocity of the swing. Among these factors, one of the most important is to generate the maximum ball velocity is the linear velocity of kicking foot's swing. Therefore, the kicker must use the dynamics of the kicking leg efficiently to generate as much kinetic energy as possible and transfer it to gain foot swing velocity. Considerable research on kinetic analysis and energy flow of the swing motion has been reported [1] [2]. However, the biomechanical mechanism by which the mechanical energy flows through the limb segments to the ball is not well explained. For this reason, a free-body power analysis of the entire limb was used to analyze the mechanical energy flow using a double pendulum model. The purpose of this study is to clarify the

1877-7058 
doi:10.1016/j.proeng.2012.04.038

mechanism used to produce the maximum velocity of the foot using mathematical analysis based on a three-dimensional double pendulum model with a moving pivot.

## 2. Double pendulum model of the kicking motion

### *2.1. The kinematics of the double pendulum*

We developed a nine degrees of freedom, dynamic double pendulum model (Fig. 1). This double pendulum model consists of two segments: the first segment freely suspended from a point in 3D space and the second suspended from the end of the first segment. The first segment (the thigh) is denoted as Link1 and the second (the shank) as Link2. It is known that the knee joint of human being rotates internally or externally in a flexed position. Therefore, we defined the knee joint as a ball joint to adopt various form of kicks. Symbols $\boldsymbol{x}_{g1}$ and $\boldsymbol{x}_{g2}$ are the positions of the center of mass in each segment. The center of the hip joint of the kicking leg is $\boldsymbol{x}_0$ and that of the supporting leg is $\boldsymbol{x}_{L0}$. The center of the knee joint is $\boldsymbol{x}_1$ and center of the foot joint is $\boldsymbol{x}_2$. Symbols $\boldsymbol{e}_{l1}$, $\boldsymbol{e}_{l2}$ are unit vectors toward the normal lines in each of the segments. Symbol $\boldsymbol{e}_{q1}$ is a cross product of $\boldsymbol{e}_{l1}$ and a vector from the knee medial to the knee lateral (this vector was named the knee axis). Symbol $\boldsymbol{e}_{q2}$ is also a cross product of $\boldsymbol{e}_{l2}$ and the knee axis. Finally, $\boldsymbol{e}_{t1}$ and $\boldsymbol{e}_{t2}$ are calculated from $\boldsymbol{e}_{l1} \times \boldsymbol{l}_{q1}$ and $\boldsymbol{e}_{l2} \times \boldsymbol{l}_{q2}$, respectively. Symbols $m$ ($m_1, m_2$), $\boldsymbol{J}$ ( $\boldsymbol{J}_1$, $\boldsymbol{J}_2$), and $l$ ($l_1$, $l_2$) are the center of mass, moments of inertia and lengths attached by Link1 and Link2, respectively. Symbols $l_{g1}$ and $l_{g2}$ are the lengths from the proximal joint to $\boldsymbol{x}_{g1}$ and $\boldsymbol{x}_{g2}$. To simplify the analysis of the system, the foot is not included in this system.

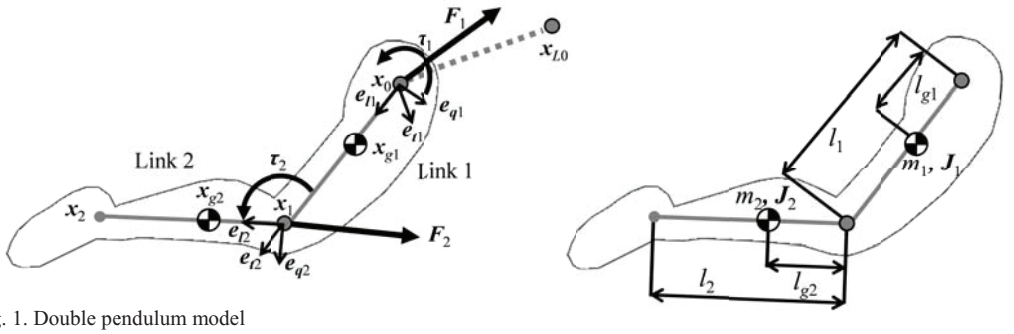


Fig. 1. Double pendulum model

Then, the acceleration vectors $\ddot{\boldsymbol{x}}_{g1}$ and $\ddot{\boldsymbol{x}}_{g2}$ are given by

$$\ddot{\boldsymbol{x}}_{g1} = \ddot{\boldsymbol{x}}_0 + \dot{\boldsymbol{\omega}}_1 \times l_{g1}\boldsymbol{e}_{l1} + \boldsymbol{\omega}_1 \times (\boldsymbol{\omega}_1 \times l_{g1}\boldsymbol{e}_{l1}) . \quad (1)$$

$$\ddot{\boldsymbol{x}}_{g2} = \ddot{\boldsymbol{x}}_1 + \dot{\boldsymbol{\omega}}_2 \times l_{g2}\boldsymbol{e}_{l2} + \boldsymbol{\omega}_2 \times (\boldsymbol{\omega}_2 \times l_{g2}\boldsymbol{e}_{l2}) , \quad (2)$$

$$= \ddot{\boldsymbol{x}}_0 + \dot{\boldsymbol{\omega}}_1 \times l_1\boldsymbol{e}_{l1} + \boldsymbol{\omega}_1 \times (\boldsymbol{\omega}_1 \times l_1\boldsymbol{e}_{l1}) + \dot{\boldsymbol{\omega}}_2 \times l_{g2}\boldsymbol{e}_{l2} + \boldsymbol{\omega}_2 \times (\boldsymbol{\omega}_2 \times l_{g2}\boldsymbol{e}_{l2}) . \quad (3)$$

### *2.2. kinemics of the double pendulum model*

The linear dynamics of each segment are

$$m_1(\ddot{\boldsymbol{x}}_{g1} - \mathrm{g}) = \boldsymbol{F}_1 - \boldsymbol{F}_2 , \quad (4)$$

$$m_2(\ddot{\boldsymbol{x}}_{g2} - \mathrm{g}) = \boldsymbol{F}_2 , \quad (5)$$

where $\boldsymbol{F}_1$ and $\boldsymbol{F}_2$ are, respectively, the force vectors acting on $\boldsymbol{x}_0$ and $\boldsymbol{x}_1$. Therefore, the joint force $\boldsymbol{F}_2$ is the internal force, the components of $\boldsymbol{F}_2$ that have an effect on the acceleration of the proximal link can be described as

$$\begin{aligned}\boldsymbol{F}_2 &= m_2(\ddot{\boldsymbol{x}}_{g2} - \boldsymbol{g}), && (6)\\ &= m_2(\ddot{\boldsymbol{x}}_0 - \boldsymbol{g}) + m_2(\dot{\boldsymbol{\omega}}_1 \times l_1\boldsymbol{e}_{l1}) + m_2(\boldsymbol{\omega}_1 \times (\boldsymbol{\omega}_1 \times l_1\boldsymbol{e}_{l1})) + \\ &\quad m_2(\dot{\boldsymbol{\omega}}_2 \times l_{g2}\boldsymbol{e}_{l2}) + m_2(\boldsymbol{\omega}_2 \times (\boldsymbol{\omega}_2 \times l_{g2}\boldsymbol{e}_{l2})). && (7)\end{aligned}$$

The rotational dynamics of each link is given by

$$\boldsymbol{J}_1\dot{\boldsymbol{\omega}}_1 + \boldsymbol{\omega}_1 \times \boldsymbol{J}_1\boldsymbol{\omega}_1 = \boldsymbol{\tau}_1 - \boldsymbol{\tau}_2 - l_{g1}\boldsymbol{e}_{l1} \times \boldsymbol{F}_1 + (l_1 - l_{g1})\boldsymbol{e}_{l1} \times (-\boldsymbol{F}_2), \quad (8)$$

$$\boldsymbol{J}_2\dot{\boldsymbol{\omega}}_2 + \boldsymbol{\omega}_2 \times \boldsymbol{J}_2\boldsymbol{\omega}_2 = \boldsymbol{\tau}_2 - l_{g2}\boldsymbol{e}_{l2} \times \boldsymbol{F}_2. \quad (9)$$

## 3. Power for each links

The kinetic energies of each link $T_1$ and $T_2$ can be described as $T_1 = 1/2 m_1 \dot{\boldsymbol{x}}_{g1}^T \dot{\boldsymbol{x}}_{g1} + 1/2 \boldsymbol{\omega}_1^T \boldsymbol{J}_1 \boldsymbol{\omega}_1$ and $T_2 = 1/2 m_2 \dot{\boldsymbol{x}}_{g2}^T \dot{\boldsymbol{x}}_{g2} + 1/2 \boldsymbol{\omega}_2^T \boldsymbol{J}_2 \boldsymbol{\omega}_2$. Also, the potential energies of each link $U_1$ and $U_2$ are $U_1 = -m_1 \boldsymbol{g}^T \boldsymbol{x}_{g1}$, $U_2 = -m_2 \boldsymbol{g}^T \boldsymbol{x}_{g2}$.

The total kinetic energy and the potential energy of Link2 is given as

$$E_2 = T_2 + U_2. \quad (10)$$

Also, the power of Link2 can be described as follows:

$$\dot{E}_2 = m_2 \ddot{\boldsymbol{x}}_{g2}^T \dot{\boldsymbol{x}}_{g2} + \dot{\boldsymbol{\omega}}_2^T \boldsymbol{J}_2 \boldsymbol{\omega}_2 - m_2 \boldsymbol{g}^T \dot{\boldsymbol{x}}_{g2} = \boldsymbol{F}_2^T \dot{\boldsymbol{x}}_1 + \boldsymbol{\tau}_2^T \boldsymbol{\omega}_2. \quad (11)$$

The total kinetic energy and the potential energy of Link1 is

$$E_1 = T_1 + U_1. \quad (12)$$

Therefore, the power of Link1 can be described as follows:

$$\dot{E}_1 = m_1 \ddot{\boldsymbol{x}}_{g1}^T \dot{\boldsymbol{x}}_{g1} + \dot{\boldsymbol{\omega}}_1^T \boldsymbol{J}_1 \boldsymbol{\omega}_1 - m_1 \boldsymbol{g}^T \dot{\boldsymbol{x}}_{g1} = \boldsymbol{F}_1^T \dot{\boldsymbol{x}}_0 - \boldsymbol{F}_2^T \dot{\boldsymbol{x}}_1 + \boldsymbol{\tau}_1^T \boldsymbol{\omega}_1 - \boldsymbol{\tau}_2^T \boldsymbol{\omega}_1. \quad (13)$$

## 4. Experiment

Ten professional male futsal players participated in this study (members from five national teams were included). Each subject preferred to kick the ball using his right leg. The subjects performed at least three maximal-effort kicking trials toward a target (10 m in front of the ball). Twenty spherical reflective markers (8 mm in diameter) were used to identify player's key anatomical landmarks. The motion of the reflective markers was recorded using a twelve-camera optoelectronic motion capture system (Vicon MXseries) at 500 Hz. The analysis phase was defined as the time from the point at which the kicking foot left the floor (-0.2 s) to one frame before impact with the ball (0.0 s). The data were smoothed by applying the bidirectional fourth-order Butterworth low-pass filter [3]. The cutoff frequency was

calculated by Yu's method [4]. In the following section, we discuss the data that was collected from one subject.

## 5. Results and discussion

### *5.1. Kinematic analysis*

$\dot{\boldsymbol{x}}_2$ (The velocity vector of $\boldsymbol{x}_2$) can be divided between $\dot{\boldsymbol{x}}_1$ (The velocity vector of $\boldsymbol{x}_1$) and $\boldsymbol{\omega}_2 \times l_2 \boldsymbol{e}_{l2}$ (the velocity due to shank rotation) and can describe as $\dot{\boldsymbol{x}}_2 = \dot{\boldsymbol{x}}_1 + \boldsymbol{\omega}_2 \times l_2 \boldsymbol{e}_{l2}$ . Fig. 2 a shows the results of $\dot{\boldsymbol{x}}_1$ , $\dot{\boldsymbol{x}}_2$ and $\boldsymbol{\omega}_2 \times l_2 \boldsymbol{e}_{l2}$ . The horizontal axis represents time of kicking motion. It shows that the ankle velocity depends on the knee velocity. However, the velocity due to shank rotation suddenly increases after the supporting foot landed and exceeds the knee velocity upon impact. It indicates that the rotation of the shank is important to produce a maximum ankle velocity. Fig.2 b shows the angular velocities of the thigh and shank. $\boldsymbol{e}_{t1}{}^T \boldsymbol{\omega}_1$ expresses the thigh's angular velocity around $\boldsymbol{e}_{t1}$ and also, $\boldsymbol{e}_{t2}{}^T \boldsymbol{\omega}_2$ expresses the shank's angular velocity around $\boldsymbol{e}_{t2}$. The peak of thigh's angular velocity occurred after the supporting leg (i.e. contralateral leg) landed. On the other hand, the peak of shank's angular velocity is observed after impact. These results suggest that it has the time lag of dynamics for the accelerating each link. Therefore, we investigated the dynamical mechanism of kicking leg in the following section.

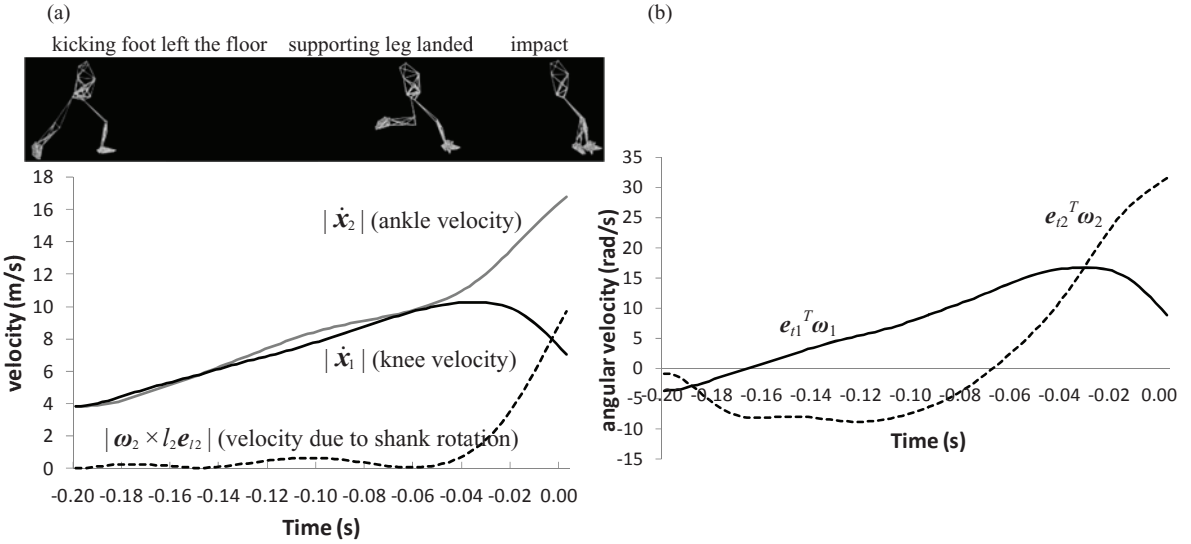


Fig. 2. (a) Comparison of components of ankle velocity; (b) comparison of angular velocity for the both segments

### *5.2. Thigh acceleration*

On the right side of Eq. (8), the second and third terms describe the effect of the acceleration of the thigh in the swing direction. Moreover, $l_{g1}(-\boldsymbol{e}_{q1}^T)\boldsymbol{F}_1$ is one of the components of $-l_{g1}\boldsymbol{e}_{l1} \times \boldsymbol{F}_1$ and it describes a moment around $\boldsymbol{e}_{t1}$ (Fig. 3 a). Fig. 3 b shows the change in the four moments around $\boldsymbol{e}_{t1}$ that affect the rotation of the thigh. In the first phase of the kicking motion, $\boldsymbol{e}_{t1}{}^T \boldsymbol{\tau}_1$ is the main cause of the increased thigh rotation; however, $l_{g1}(-\boldsymbol{e}_{q1}^T)\boldsymbol{F}_1$ gained after the supporting leg contacted the floor, also contributes to the increase. It was thought that the increase in the $l_{g1}(-\boldsymbol{e}_{q1}^T)\boldsymbol{F}_1$ value was primarily caused by the impact force ($\boldsymbol{F}_{\text{brake}}$) of the landing of the supporting leg (-0.06 s) being transferred to the pelvis.

Then the acceleration of the thigh increased by $l_{g1}(-\boldsymbol{e}_{q1}^{T})\boldsymbol{F}_1$. This method of acceleration that uses a sudden stop is called the "braking effect" in this study.

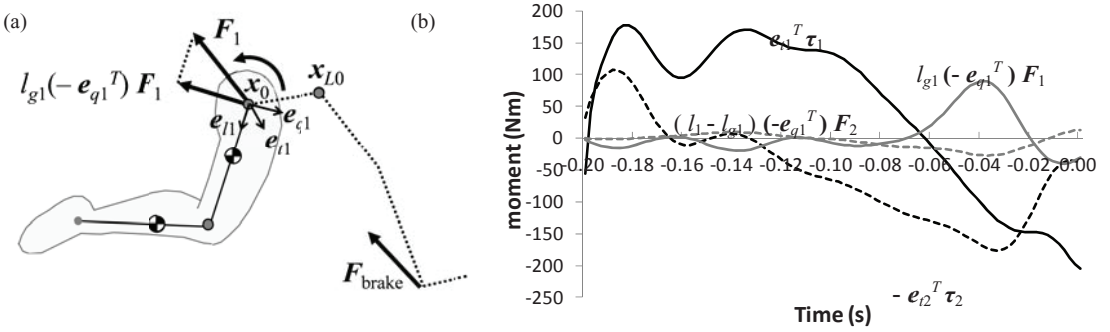


Fig. 3. (a) Braking force of hip joint; (b) components of rotation torque in Link1

*5.3. Shank acceleration*

Using the multi-body power analysis [5], we discuss how the non-muscular forces act to increase energy in order to produce the maximum swing velocity. The internal force $\boldsymbol{F}_2$ and $\dot{\boldsymbol{x}}_1$ (which is the velocity vector of $\boldsymbol{x}_1$) can express $\boldsymbol{F}_2 = [F_{q2}, F_{t2}, F_{l2}]^T$ and $\dot{\boldsymbol{x}}_1 = [{}^1\dot{x}_{q2}, {}^1\dot{x}_{t2}, {}^1\dot{x}_{l2}]^T$. Using this equation, $\dot{E}_2$ can be described as

$$\dot{E}_2 = \overbrace{\boldsymbol{F}_2^T\dot{\boldsymbol{x}}_1}^{} + \boldsymbol{\tau}_2^T\boldsymbol{\omega}_2, \tag{14}$$

$$= \overbrace{F_{t2}^1\dot{x}_{t2}}^{{}^{t2}P} + \overbrace{F_{l2}^1\dot{x}_{l2}}^{{}^{t2}P} + \overbrace{F_{q2}^1\dot{x}_{q2}}^{{}^{q2}P} + \boldsymbol{\tau}_2^T\boldsymbol{\omega}_2. \tag{15}$$

Then, we observed that the main component of $\boldsymbol{F}_2$ is the centrifugal force. Therefore, by substituting Eq. (7) in ${}^{t2}P \equiv F_{l2}^1\dot{x}_{l2} \equiv (\boldsymbol{e}_{l2}^T\boldsymbol{F}_2)(\boldsymbol{e}_{l2}^T\dot{\boldsymbol{x}}_1)$, we obtain

$$\begin{aligned} {}^{t2}P &\equiv F_{l2}^1\dot{x}_{l2}, \\ &= \underbrace{m_2{}^1\dot{x}_{l2}\boldsymbol{e}_{l2}^T\{\ddot{\boldsymbol{x}}_0 - \boldsymbol{g}\}}_{{}^{t2}P_{lin}} + \underbrace{m_2{}^1\dot{x}_{l2}\boldsymbol{e}_{l2}^T\{\dot{\boldsymbol{\omega}}_1 \times l_1\boldsymbol{e}_{l1}\}}_{{}^{t2}P_{L1a}} + \underbrace{m_2{}^1\dot{x}_{l2}\boldsymbol{e}_{l2}^T\{\boldsymbol{\omega}_1 \times (\boldsymbol{\omega}_1 \times l_1\boldsymbol{e}_{l1})\}}_{{}^{t2}P_{L1c}} + \\ &\underbrace{m_2{}^1\dot{x}_{l2}\boldsymbol{e}_{l2}^T\{\dot{\boldsymbol{\omega}}_2 \times l_{g2}\boldsymbol{e}_{l2}\}}_{{}^{t2}P_{L2a}} + \underbrace{m_2{}^1\dot{x}_{l2}\boldsymbol{e}_{l2}^T\{\boldsymbol{\omega}_2 \times (\boldsymbol{\omega}_2 \times l_{g2}\boldsymbol{e}_{l2})\}}_{{}^{t2}P_{L2c}}. \end{aligned} \tag{16}$$

Here, ${}^{l2}P_{lin,}$ ${}^{l2}P_{L1a,}$ ${}^{l2}P_{L1c,}$ ${}^{l2}P_{L2a}$ and ${}^{l2}P_{L2c}$ are the components of linear acceleration, angular acceleration of the thigh, centrifugal acceleration of the thigh, angular acceleration of the shank, and centrifugal acceleration of the shank respectively. Fig. 3 shows the change in these power components that have an effect on the energy of the shank. Symbols ${}^{l2}P_{lin}$ and ${}^{l2}P_{L1a}$ show the low values compared with others. On the other hand, ${}^{l2}P_{L1c}$ and ${}^{l2}P_{L2c}$ show higher values before impact. Furthermore, $\boldsymbol{F}_2{}^T\dot{\boldsymbol{x}}_1$ is the inner product of $\boldsymbol{F}_2$ and $\dot{\boldsymbol{x}}_1$. Therefore, when the subject places his knee at an angle of 90 degrees, the energy from the thigh could be effectively transferred to the shank (Fig. 4). In the experiment, the subject kept his knee

angle close to 90 degrees at the peak of the thigh's angular acceleration. In other words, the shank was accelerated by the energy produced by the thigh and effectively transferred to the shank by the internal force of the action. Moreover, the knee extension torque was the main contributor to the increase in swing velocity after the supporting leg landed.

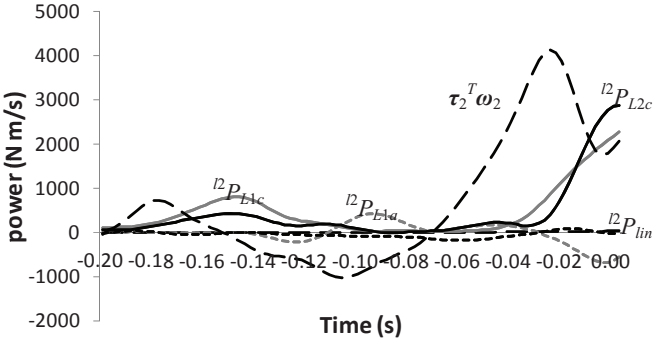


Fig. 3. Sources of power for Link2

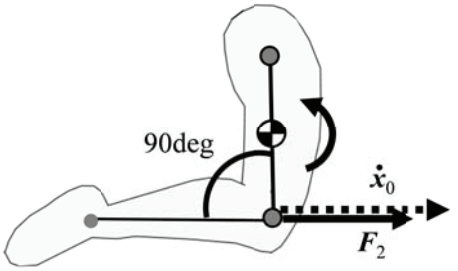


Fig. 4. The idealized posture for an effective energy transfer

## Conclusion

We investigated how the non-muscular forces generate, absorb, and transfer energy in order to produce the maximum swing velocity of the leg. The dominant force to accelerate the thigh was the muscle force generated by the hip extension torque. Following this energy production, the braking effect contributed to the increase after the supporting leg landed. On the other hand, the shank was accelerated by the muscle force generated from the knee extension torque at approximately the same time as the braking effect. Finally, the non-muscular forces generated by the thigh action contributed to increase the ankle velocity. It was thought that the subject controlled their motion of kicking leg skilfully to transfer the energy effectively.

## References

[1] Zajac, F.E., Neptune, R.R., Kautz, S.A., 2002. Biomechanics and muscle coordination of human walking. part I: introduction to concepts, power transfer, dynamics and simulations. Gait & Posture Vol. 16, No. 3: 215–232.

[2] Nunome, H., Asai, T., Ikegami, Y., Sakurai, S., 2002. Three-dimensional kinetic analysis of side-foot and instep soccer kicks. Med Csi Sports Exerc 34 (12): 2028–2036.

[3] Winter, A D., 1990. Biomechanics and motor control of human movement. Second edition. John Wiley & Sons, New York, pp. 41–43.

[4]Yu, B., Gabriel, D., Noble, L., An, K. N., 1999. Estimate of the Opitimum Cutoff Frequency for the Butterworth Low-Pass Digital Filter. JOURNAL OF APPLIED BIOMECHANICS 15: 318–329.

[5] Ohta, K., Ohgi, Y., Shibuya, K., 2011. Multi-body power analysis of golf swing based on a double pendulum with moving pivot. Procedia Engineering: 9th Conference of the International Sports Engineering Association (ISEA).